

Electron and Carbon Balances in Microbial Fuel Cells Reveal Temporary Bacterial Storage Behavior During Electricity Generation

STEFANO FREGUIA, KORNEEL RABAEY, ZHIGUO YUAN, AND JÜRGE KELLER*

Advanced Wastewater Management Centre, The University of Queensland, St. Lucia, QLD 4072, Australia

Microbial fuel cells (MFCs) are emerging as a novel technology with a great potential to reduce the costs of wastewater treatment. Their most studied application is organic carbon removal. One of the parameters commonly used to quantify the performance of these cells is the Coulombic efficiency, i.e., the electron recovery as electricity from the removed substrate. However, the "inefficiencies" of the process have never been fully identified. This study presents a method that uses the combination of electrochemical monitoring, chemical analysis, and a titration and off-gas analysis (TOGA) sensor to identify and quantify the sources of electron loss. The method was used successfully to close electron, carbon, and proton balances in acetate and glucose fed microbial fuel cells. The method revealed that in the case that a substrate is loaded as pulses carbon is stored inside the cells during initial high substrate conditions and consumed during starvation, with up to 57% of the current being generated after depletion of the external carbon source. Nile blue staining of biomass samples revealed lipophilic inclusions during high substrate conditions, thus confirming the storage of polymeric material in the bacterial cells. The method also allows for indirect measurement of growth yields, which ranged from 0 to 0.54 g biomass-C formed per g substrate-C used, depending on the type of substrate and the external resistance of the circuit.

Introduction

Recently, increasing attention has been dedicated to microbial fuel cells (MFCs). MFCs are an attractive technology because they can achieve organic carbon removal while recovering useful energy in the form of electricity. Briefly, MFCs are fuel cells in which bacteria perform the role of anodic catalyst. Hence, the electron transfer from an electron donor (typically a reduced organic molecule) to the anode is catalyzed by an anodophilic biofilm which grows on the anodic electrode surface (1). The electrons then flow through an external resistor or power user before ultimately reducing an electron acceptor at the cathode. The most sustainable electron acceptor is oxygen. Many studies focused on the anode have used potassium ferricyanide ($K_3Fe(CN)_6$) as a chemical electron acceptor. While this compound is not

sustainable in its use and not suited for practical applications, its low cathodic overpotential and thus its ability to provide a constant cathodic potential make it ideally suited to enable research on the anodic processes (2). The electrical circuit of an MFC is closed by the diffusion of protons and/or other cations from anodic to cathodic compartment through a cation exchange membrane (CEM).

The research done to date on microbial fuel cells has addressed two main areas: (i) understanding the microbial diversity of anodophilic communities and the pathways of electron transfer (3–5); (ii) increasing the power output of the cells through different strategies, such as improving the anode and cathode materials (6) and decreasing the internal resistance of the cells (7, 8). The MFC performance has been reported through parameters such as power density (W/m^2 anode surface or W/m^3 anode liquid volume), organic loading rate ($kg_{COD}/m^3 d$), and Coulombic efficiency. The Coulombic efficiency is defined as the ratio of total Coulombs transferred to the anode from the substrate, to the maximum possible Coulombs if all substrate removed produced current (9). Unfortunately, the Coulombic efficiency only provides one part (current production) of the overall electron balance. All the electrons that are not transferred to the anode have so far been considered simply as losses, but the nature of these losses has not been identified or specifically quantified in depth through detailed mass or charge balances. Possible sinks of electrons include methanogenesis, hydrogen production by fermentation, oxidation by electron acceptors other than the anode (such as oxygen, sulfate, or nitrate), and bacterial growth. The goal of this study has been to develop and validate a method for the identification and quantification of the electron losses that occur in microbial fuel cells. Such a method requires continuous monitoring of current generation and gas production. Method development and validation were carried out under strictly controlled conditions with acetate and glucose as the sole electron donors.

Materials and Methods

Microbial Fuel Cells. Two double-chamber microbial fuel cells built in rectangular geometry were used for the experiments. The volume of both the anodic and cathodic compartments was 480 cm^3 , each with a headspace of 44 cm^3 . Both compartments were filled with granular graphite (El Carb 100, Graphite Sales, Inc., USA). The granules were 2–6 mm in diameter and had a porosity of 45%, leaving a liquid volume of 200 mL in each compartment. At the anode, the granular matrix served as biofilm support and conducting matrix, conveying electrons to a graphite rod. At the cathode, the graphite carried electrons to the final electron acceptor, which in this study was an unbuffered 150 mM potassium ferricyanide ($K_3Fe(CN)_6$) solution. The anodic and cathodic rods were connected through an external resistor with variable resistance (maximum 100 Ω) to close the circuit. Two Ag/AgCl reference electrodes (Ref 201, Radiometer Analytical) were placed in the anodic and cathodic compartments of each cell and connected to the respective electrodes, for measurements of half-cell potentials. The cation exchange membrane (CEM) was made of Ultrex (CMI-7000, Membranes International, USA). The anodic solution was recirculated at a rate of approximately 200 mL/min to maintain well mixed conditions and to avoid concentration gradients and clogging of the granular matrix. The catholyte was pumped around the granular bed to reduce cathodic concentration polarization. The anolyte consisted of modified M9 medium with the following composition: 6 g/L NaH_2-

* Corresponding author phone: +61 7 3365 4727; fax: +61 7 3365 4726; e-mail: j.keller@awmc.uq.edu.au.

PO₄, 3 g/L KH₂PO₄, 0.1 g/L NH₄Cl, 0.5 g/L NaCl, 0.1 g/L MgSO₄·7H₂O, 15 mg/L CaCl₂·2H₂O, and 1.0 mL/L of a trace elements solution as previously described (10). The reactors and the related tubing were thoroughly wrapped in aluminum foil to exclude light. Two types of biomass were used in the experiments, one adapted to acetate and one adapted to glucose. The adaptation was achieved over more than 6 months of continuous feeding of the respective substrate at a loading rate of approximately 1 kg_{COD}/m³ d. The adaptation resulted in a continuous power generation of approximately 100 W/m³ anode liquid volume.

Electrochemical Monitoring. The anode and cathode of each MFC were connected to an Agilent 34970A data acquisition unit. Voltage data were collected every 20 s. The current was deduced from the external resistance using Ohm's law. The charge transferred to the circuit over time was calculated by integrating the current with respect to time. The Ag/AgCl reference electrodes were also connected to the instrument. The reading of the voltages between reference electrodes and operating electrodes was a measurement of anodic and cathodic half-cell potentials.

Titration and Off-Gas Analysis (TOGA). The TOGA sensor system as developed by Pratt et al. (11) was used to determine gas production rates and proton (H⁺) production rate (PPR) at the anode of the reactors described above. The TOGA sensor consists of (1) a bioreactor, where batch experiments under controlled operational conditions can be carried out; (2) a pH controller to accurately control the pH during an experiment at a pre-specified set-point, and through which the proton production/consumption rate caused by the biological and physicochemical processes occurring in the bioreactor can be quantified; and (3) an off-gas measurement arrangement involving the use of a mass spectrometer (Omnistar, Balzers AG, Liechtenstein), and several mass flow controllers and meters to determine the transfer rates of gaseous compounds of interest through gas-phase mass balance. A full description of the TOGA principles can be found in studies by Pratt et al. and Gapes et al. (11, 12), while the use of the TOGA sensor in this study is further described in the following section.

Batch Tests. The reactors were connected to the TOGA sensor and operated in batch mode to calculate electron, carbon, and H⁺ balances around the anodic compartments. Before starting any of the experiments, the routine continuous feeding was stopped and the reactor was operated overnight in starvation conditions (no feed addition) and flushed with He (100 mL/min) with pH controlled at 7.0 ± 0.01. This was done to fully deplete any leftover substrate (which was verified by chemical analysis before injection of new substrate) and to strip out CO₂ that might have accumulated in the reactor. Any current produced by the reactor after overnight starvation was attributed to endogenous processes and subtracted from the total current during the batch to obtain the exogenous current. While this assumption may be challenged, it is necessary to make as there is no possibility to determine the COD utilization under endogenous conditions, and hence the associated current should not be included in the overall electron balance either. It was assumed that the endogenous processes occurred at a constant rate during the whole batch. The endogenous current accounted for 7% (at 5 Ω external resistance) to 53% (at 100 Ω external resistance) of the total charge transferred to the anode during the batch experiment. Before substrate injection, the stripping Helium flow rate was boosted to 250 mL/min to achieve quicker stripping of the CO₂ produced by the bioreactions. The Helium flow would also strip any methane (CH₄) and hydrogen (H₂) produced. The feed solution contained substrate (acetate or glucose, 0.4–2.3 g_{COD}/L), NH₄Cl (0.2 g/g_{COD}), and trace elements and was injected rapidly as a concentrated solution into the test cell at the beginning of the experiment. Acetate was fed only into

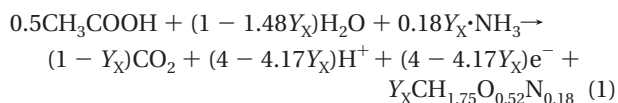
the reactor containing an acetate-adapted biofilm; glucose was used with both the acetate-adapted and glucose-adapted biofilms. The injection volume was 10 mL. The concentrations were chosen according to the external resistance of the circuit to obtain comparable cycle times. Batch experiments were operated at 5, 20, and 100 Ω. At smaller resistances the currents are higher and larger quantities of substrate are necessary to generate a complete potential profile and to minimize substrate limitation. The substrate was dosed to obtain initial chemical oxygen demand (COD) concentrations in the reactor of approximately 120 mg/L at 5 Ω, 60 mg/L at 20 Ω, and 20 mg/L at 100 Ω. In all the tests the pH was kept at 7.0 ± 0.01 and the temperature remained constant at 22 ± 1 °C. During the batch tests, the cell voltage was continuously recorded with the data acquisition unit mentioned above; the carbon dioxide transfer rate (CTR), the CH₄ and H₂ transfer rates, and the PPR signal were continuously recorded by the TOGA. Liquid samples were taken periodically and analyzed for volatile fatty acids (VFA) or soluble chemical oxygen demand (COD), respectively, when acetate and glucose were used as substrates. The batches were terminated when the current leveled back to the endogenous level. Each cycle was repeated at least three times to examine reproducibility of the results.

Chemical Analysis. Liquid anolyte samples were filtered with a 0.22 μm filter and analyzed for volatile fatty acids (VFAs) or chemical oxygen demand (COD). For VFA analysis, 0.9 mL of sample was added to 0.1 mL of 10% formic acid and subsequently analyzed with a gas chromatography method using a polar capillary column (DB-FFAP) at 140 °C and a flame ionization detector at 250 °C. The COD measurements were done according to the dichromate method (13).

To analyze the elemental composition of the biomass, a sample (approximately 20 mg) was collected from the reactor effluent after a short process upset (caused by a sudden pH increase). The biomass was pelleted by centrifugation, fixed with paraformaldehyde, washed with a phosphate buffer, and subsequently freeze-dried. The dried sample was then analyzed with a Carlo Erba NA-1500 elemental analyzer.

Reactions and Balance Equations. The first step in creating a robust method to close balances around the reactor is to identify all the reactions putatively occurring at the anode. Reaction 1 describes the bioelectrochemical process for the direct oxidation of acetate. The biomass formula was obtained by analyzing the elemental composition of a dried biomass sample from the reactor, as described above. It is assumed that between cycles the biomass composition can be regarded as constant. However, depending on the growth phase and any storage compounds present this composition can vary. In the equation, Y_X is the growth yield of biomass, expressed as the ratio of C-moles of biomass formed to C-moles of reacted substrate.

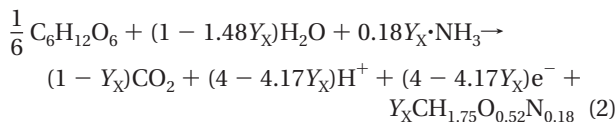
Acetate direct oxidation occurs as follows:



Acetate could also be the substrate for acetate utilizing methanogens, which can convert it to methane and carbon dioxide. However, methane production from acetate was not observed at any of the test conditions, so this reaction was not included in this model. Reaction 2 describes the bioelectrochemical oxidation of glucose. With glucose, fermentation can occur (reaction 3). Acetate is produced by fermentation and can be utilized for current generation according to reaction 1. The hydrogen produced by fermentative processes can be used by methanogens to produce

methane gas (reaction 4) or used directly by anodophilic bacteria for transfer of electrons to the electrode (reaction 5). Reaction 3 is only one of several types of fermentation that can occur in the anaerobic anodic compartment. Fermentations can also produce higher VFAs such as propionate or butyrate and these were also monitored by chemical analysis to close electron and carbon balances. However, no net accumulation of higher VFAs was observed in any of the tests. A total COD measurement furthermore supplied a control for carbon possibly exiting in other forms.

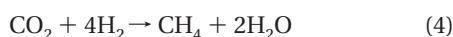
Glucose direct oxidation:



Glucose fermentation:



Methanogenesis:



Direct hydrogen oxidation:



A batch test is analyzed here as a dynamic closed system where all inputs and outputs are measured and some reactor-internal concentrations (VFA, COD) are determined regularly. Three independent equations were identified to link all the variables of the process. These are the electron balance, the carbon balance, and the proton balance, shown in their integral form in eqs 6, 7, and 8a/8b, respectively.

Electron balance:

$$0 = \gamma_s \cdot \Delta S - \frac{3,600Q}{F} - 8 \cdot \Delta CH_4 - 2 \cdot \Delta H_2 - 4.17 \cdot \Delta X \quad (6)$$

Carbon balance:

$$0 = \Delta S - \Delta CO_2 - \Delta CH_4 - \Delta X \quad (7)$$

Proton balance (acetate):

$$PP = \frac{3,600Q}{F} - \frac{0.5\Delta S}{1 + 10^{pK_{a,ac}-pH}} + \frac{\Delta NH_3}{1 + 10^{pK_{a,NH_4^+}-pH}} \quad (8a)$$

Proton balance (glucose):

$$PP = \frac{3,600Q}{F} + \frac{\Delta NH_3}{1 + 10^{pK_{a,NH_4^+}-pH}} \quad (8b)$$

In the equations, ΔS is the substrate consumption over a batch (C-mmol), γ_s is the degree of reduction of the substrate (4 for both acetate and glucose), Q is the charge transferred to the external circuit (mCoulomb), F is the Faraday constant (96,485 mCoulomb/mmol), ΔX is the biomass growth over a batch (C-mmol), and 4.17 is the degree of reduction of biomass. The biomass growth is related to the previously defined Y_X (observed yield) through eq 9.

$$\Delta X = Y_X \cdot \Delta S \quad (9)$$

PP is the proton production (mmol H^+) and ΔNH_3 (mmol) is the ammonia consumed for biomass growth. ΔCO_2 , ΔCH_4 ,

and ΔH_2 (all expressed in mmol) are the carbon dioxide, methane, and hydrogen gas productions over the complete experiment, respectively. Due to the very low solubility of methane and hydrogen in the anolyte, the high inert gas flow through the anode compartment for stripping, and the turbulence induced by recirculation, no temporary accumulation in the liquid phase is expected for these two gases. For CO_2 this may not be true due to the high solubility of this gas in water. The production rate of CO_2 is equal to the transfer rate plus any CO_2 accumulation in the liquid phase. The CO_2 accumulation is normally not negligible, especially during transient conditions. However, analysis of liquid anolyte samples (stripping in acidic solution followed by detection by a mass spectrometer) revealed that the total inorganic carbon concentration of the liquid phase at the beginning and at the end of the batches was consistently low (typically 10–20 mg/L) and not varying appreciably. It was therefore assumed that over a whole batch no net accumulation of CO_2 could occur, thereby setting the CO_2 production over the whole batch equal to the CO_2 transfer.

Equation 6 is an electron balance, which reflects the fact that the only electron sinks can be current, methane, hydrogen, and biomass. Equation 7 is the carbon balance which reflects that the only carbon outputs are CO_2 , CH_4 , and biomass. Equation 8 (H^+ balance) implicates that H^+ can be produced by the current generating reactions (reactions 1, 2, and 5), or by the shift of the acid/base equilibria of the acetate/acetic acid buffer and NH_3/NH_4^+ buffer. The former effect is present only if the substrate can be ionized and it reflects that any molecule of acetic acid taken up by the biomass will cause the protonation of some acetate to respect the pK_a of this equilibrium; the latter reflects a similar effect due to ammonia uptake by the bacteria for growth. Ammonium diffusion through the CEM has a negligible pH effect as long as the pH in the reactor is much lower than the pK_a of the NH_3/NH_4^+ equilibrium (i.e., $pH \ll 9.2$). More on these effects is explained in refs 11, 12. Equation 8 also assumes that the protons do not diffuse through the CEM during the batch tests. This assumption was backed by the fact that the pH at the cathode did not vary for the duration of the experiments. The neutralization of any H^+ produced at the anode by the pH controller appeared to be faster than any H^+ diffusion through the CEM.

All the variables in the three balance equations are measured, except ΔX , or equivalently the growth yield Y_X . Due to the low measurement error of the variables involved in the electron balance (Q and the ΔS), this equation was chosen to calculate ΔX . The carbon balance and the PP balance hence provided independent equations to check the validity of the method.

Results

Balances in Acetate-Fed Microbial Fuel Cells. Offgas analysis revealed that no methane or hydrogen production occurred with this non-fermentable substrate. The only possible electron sink other than current generation is microbial growth. The calculation of ΔX from the electron balance (eq 6) revealed a dependence of the growth yield on the external resistance. As shown in Figure 1, the growth yield decreases as the external resistance increases, with values (in units of C-mol biomass/C-mol substrate \pm standard deviation) of 0.304 ± 0.040 at 5 Ω , 0.237 ± 0.019 at 20 Ω , and -0.016 at 100 Ω (this implies stoichiometric conversion of substrate to current).

Table 1 shows the main measured variables for each condition, as well as the errors of the carbon and proton balances. These errors were calculated by dividing the equation residuals by ΔS and PP for the carbon and H^+ balance, respectively. The errors in PP balance are all less than 10%, which shows a good correlation between the

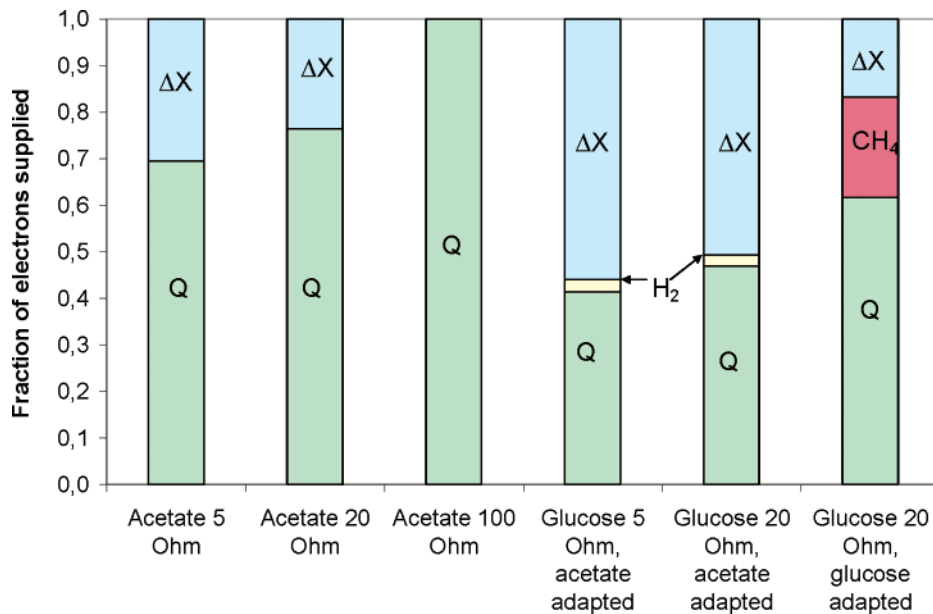


FIGURE 1. Breakdown of electron consumption among the different electron sinks (Q = electrons transferred to the anode, ΔX = electrons diverted to biomass growth).

TABLE 1. Summary of Batch Test Results for Acetate and Glucose Fed Microbial Fuel Cells

	cycle time (min)	substrate dosing (C-mmol)	ΔS (C-mmol)	Q/F (mmol e ⁻)	ΔCO_2 (mmol)	ΔH_2 (mmol)	ΔCH_4 (mmol)	ΔX (C-mmol)	error on C balance	error on H ⁺ balance
acetate 5 Ω	108 ± 7	0.732	0.730 ± 0.007	2.029 ± 0.109	0.623 ± 0.029	0.0	0.0	0.213 ± 0.029	14.5%	10.0%
acetate 20 Ω	177 ± 3	0.379	0.374 ± 0.009	1.125 ± 0.056	0.318 ± 0.063	0.0	0.0	0.089 ± 0.011	8.8%	7.5%
acetate 100 Ω	1053	0.254	0.235	1.007	0.187	0.0	0.0	-0.016	20.4%	3.5%
glucose ^a 5 Ω	217 ± 6	0.751	0.752 ± 0.000	1.246 ± 0.104	0.380 ± 0.009	0.03 ± 0.005	0.0	0.403 ± 0.023	4.1%	6.8%
glucose ^a 20 Ω	153 ± 15	0.379	0.373 ± 0.027	0.714 ± 0.040	0.159 ± 0.020	0.018 ± 0.003	0.0	0.178 ± 0.032	9.7%	1.9%
glucose ^b 20 Ω	158 ± 8	0.378	0.378 ± 0.000	0.940 ± 0.090	0.380 ± 0.015	0.0	0.041 ± 0.008	0.061 ± 0.037	27.5%	6.2%

^a Acetate-adapted consortium. ^b Glucose-adapted consortium.

measured current and H⁺ production rate. The carbon balance has somewhat larger errors (9–20%). This is possibly due to the error caused by the assumption of a constant endogenous CO₂ production, especially at the high external resistance of 100 Ω , when endogenous processes account for more than 50% of the current production. In a control experiment (not shown), the system was operated in open circuit; at this condition some CO₂ (but no H₂ or CH₄) production was observed. Upon closing the circuit, the current generated accounted for a similar electron recovery as in the cases in which the circuit was closed throughout the experiment. This suggests that no significant net loss to an alternative electron acceptor had occurred during the open circuit experiment.

Balances in Glucose-Fed Microbial Fuel Cells. The results detailed in Table 1 show that the method could, in most cases, reasonably close the balances even for a fermentable substrate such as glucose. Hydrogen production was detected with acetate-adapted biomass, methane generation was instead observed with glucose-adapted biomass. The growth yields on glucose as calculated from the electron balance were higher compared to the growth yields on acetate, namely 0.495 ± 0.057 and 0.559 ± 0.031 C-mol biomass/C-mol substrate for the 20 Ω and 5 Ω batches with acetate-adapted biomass. The glucose-adapted biomass only produced 0.114 ± 0.102 C-mol biomass/C-mol substrate for a resistance of 20 Ω .

Dynamic Behavior of Acetate-Fed Microbial Fuel Cells. An analysis of the batch profiles revealed the dynamics of

substrate uptake and utilization by anodophilic bacteria in microbial fuel cells. The electron balance was used in its instantaneous form.

$$0 = 4r_s - \frac{3,600I}{F} - 4.17r_x - 4.50r_p \quad (10)$$

In the equation the terms have the units of rates: r_s is the substrate uptake rate (C-mmol/hr), I is the current (mA), r_x is the biomass growth rate (C-mmol/hr). The methane production rate and hydrogen production rate were eliminated from the equation, because they are negligible with acetate as the substrate. A new term (r_p , C-mmol/hr) was added to include the possibility of carbon storage inside the cells. This new term was necessary to explain the profiles observed in the acetate-fed batches. Bacteria commonly are able to take up external substrates and store them in the form of polymers when the substrate is in excess. Storage polymers can then be used as carbon and energy sources during starvation. The most common storage polymers are poly- β -hydroxyalkanoates (PHAs) and glycogen. When acetate is the carbon source, poly- β -hydroxybutyrate (PHB) is normally the only storage polymer observed (14). The coefficient 4.50 in eq 10 represents the degree of reduction of PHB.

PHB is formed from acetate according to reaction 11 and it can be used as a carbon and electron source when the external substrate is depleted (reaction 12). Current production from PHB is accompanied by growth of biomass with

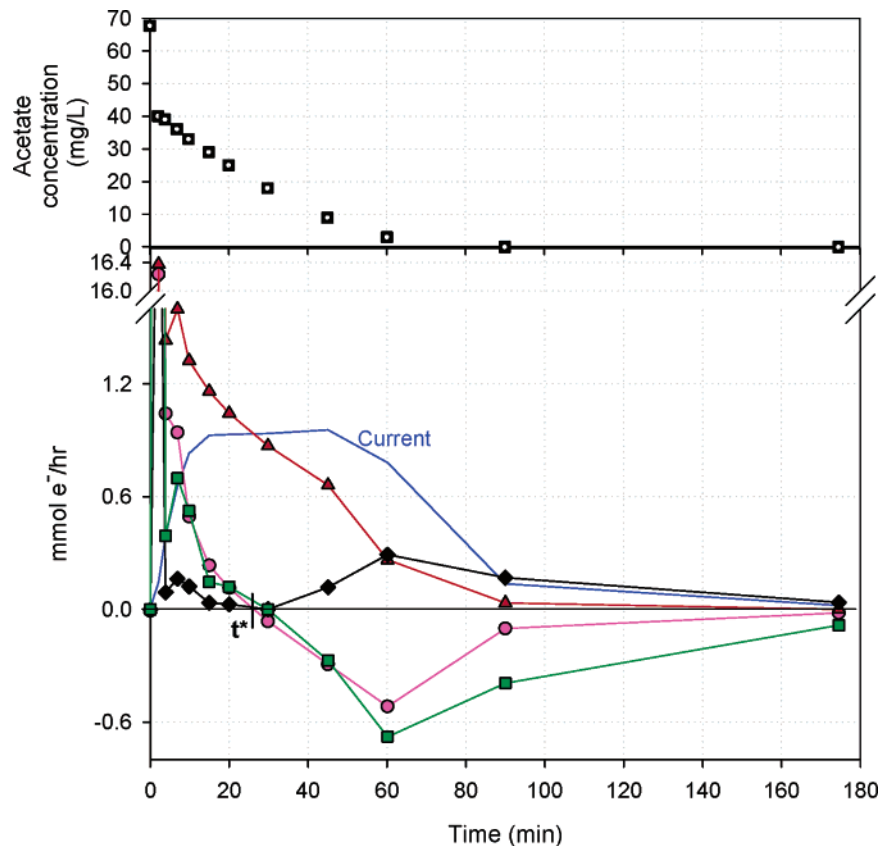
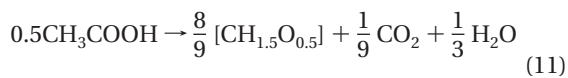


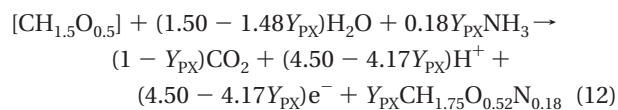
FIGURE 2. Profiles of electron source and sinks for acetate-fed batch, 20 Ω : (\blacktriangle) substrate consumption rate; (unmarked line) current generation; (\bullet) electrons used for bacterial growth and storage; (\blacklozenge) electron uptake for growth; (\blacksquare) electrons used for PHB storage or delivered by PHB oxidation (t^* is the time when the storage process stops and the current starts to be generated from storage products). The top portion of the graph shows the acetate concentration in the reactor (\square).

yield Y_{PX} (C-mol biomass/C-mol substrate), as shown in the equation.

PHB storage



PHB oxidation



The terms r_X and r_P cannot be distinguished experimentally unless biomass sampling and analysis is carried out. However, representative biomass sampling can be difficult when bacteria grow in a thin biofilm. The goal of this study was to develop a method to estimate these terms without the need of direct biomass measurements. The combined term $4.17r_X + 4.50r_P$ represents the electrons that are diverted internally to the bacterial cells, either for synthesis of new biomass or for storage of PHB; r_X is always positive, whereas r_P is positive during PHB accumulation and negative during PHB consumption for current production and growth. It must be noted that eq 10 is valid during both PHB accumulation and consumption.

Figure 2 shows the profiles of electron source (acetate) consumption rate and electron uptake rate by the different sinks (current, growth, and storage) for the 20 Ω batch experiment. An initial very fast uptake of substrate is observed. The current production rises more slowly and maintains a nearly constant value for most of the batch. The internal

diversion of electrons initially follows the substrate uptake rate, but in the second half of the batch it assumes negative values. This can only be explained by admitting a storage process. A theoretical approach was used to distinguish the growth and storage effects. The approach is based on the theories developed by van Aalst-van Leeuwen (14) and Pratt (11). This approach is based on energy considerations and allows for the calculation of r_X and r_P . The theory is described in more detail in the Supporting Information. The above-mentioned calculation shows that depending on the applied resistance a significant portion of the total growth in a batch occurs on PHB (34% at 5 Ω , 65% at 20 Ω , and no growth at 100 Ω). Also it appears that, as the external resistance increases, an increasing fraction of the total charge delivered to the external circuit derives from PHB: 25% at 5 Ω , 49% at 20 Ω and 57% at 100 Ω .

Storage polymer formation is also suggested by the profile of the anodic potential, shown in Figure 3. The anodic potential quickly decreased after substrate injection, then reached a stable level around -140 mV SHE, for 15 min. Then the potential started decreasing further to a lower level of -170 mV SHE. This indicates that after 30 min from the start of the batch the electron donor became more reduced. This is likely due to the shift from acetate to PHB as electron donor for the anodic oxidation. As shown in the figure, the time when the anodic potential started to decrease from -140 mV to -170 mV corresponds to the time when the rate of storage, as calculated by theoretical calculation, became negative, i.e., the storage product started to be used as substrate for current generation. This reinforces the hypothesis of the correlation between storage of PHB and anodic potential. The visualization of polymeric inclusions within the bacterial cells at high substrate concentration is the third

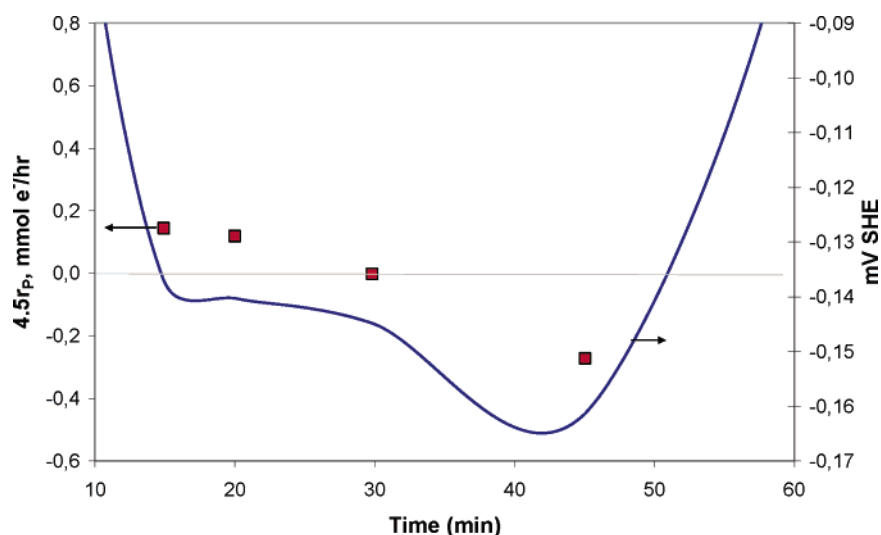


FIGURE 3. Electron consumption for storage (□) and anodic potential vs standard hydrogen electrode (solid line) during the phase when the storage process stops and the storage polymer starts to be used as substrate for current generation.

proof that a storage process is indeed occurring. More information on the method and results can be found in the Supporting Information.

Discussion

Method Development. Limited work has been carried out to date to identify the efficiency losses observed within the MFC process. In this work, we proposed and demonstrated a method to gain a more detailed understanding of the biological reactions occurring in the anodic compartment. The method can (1) establish which biochemical reactions are happening in the system and their extent; (2) identify and quantify the “inefficiencies” or electron losses of the process; (3) estimate growth rates and polymer storage rates; (4) close electron, carbon, and proton balances. Once a set of possible biochemical reactions is identified for the system, the balances can be applied over a whole batch to determine whether the proposed set is an accurate representation of the actual processes occurring in the MFC. When applied to microbial fuel cells fed with acetate or glucose, the balances were closed with an error which, in most cases, was less than 10%. Also, the biomass growth yield was estimated with an error of 10% or less. If other processes (chemical transformations or physical processes) were taking place in the system at significant rates, the balances would not be closed within the error margin. For example, if there was significant oxygen infiltration in a reactor, this would be detected as an electron imbalance, as electrons would be diverted from the electrode. Also ferricyanide diffusion can likewise be excluded as a significant process.

The estimation of growth yields and storage rates of polymers is of great importance to understand the dynamics of carbon uptake and usage by MFC biofilms. The continuous quantification of these variables without the need of direct measurements is particularly useful in MFCs. Accurate measurements of biomass growth rates are inherently difficult in biofilm systems, and even more so in MFCs where the representative sampling of biomass is generally not possible without opening the MFC and therefore severely interrupting the MFC operation.

Even though the method was tested only with defined substrates in the absence of alternative electron acceptors at the anode, its validity is not limited to these conditions as it can be applied without substantial modifications to a variety of electron donors and in the presence of electron acceptors such as nitrate and oxygen.

Biomass Growth and Storage of PHB. The results indicate that the observed biomass growth yields are higher at lower external resistances. The reason for this trend can be found in the increased energy gain for the bacteria at low resistance. For a set current, the voltage generated over the resistor is lower, which implies a higher anodic potential. As the potential of the anode as electron acceptor determines the bacterial yield through the energy gain per electron transferred, a higher potential creates more opportunity for growth (15). Data on anodic potentials can be found in the Supporting Information. An MFC operating at 5 Ω provides an extra 200 mV for bacterial growth compared to an MFC operating at 100 Ω.

When glucose is the electron donor, the energy gain for the bacteria is higher than with acetate, due to the lower standard potential of glucose (−429 mV SHE at pH 7 compared to −287 mV SHE for acetate at pH 7). The growth yields are therefore higher, as confirmed in Table 1. However, the low growth yield observed with the glucose-adapted biofilm cannot be explained based solely on energy considerations. Functionality shifts certainly played a role in this case.

Like many other heterotrophic bacteria, anodophilic bacteria in MFCs are able to store carbon, likely in the form of PHAs. The data obtained in this study indicate that the fraction of current produced through PHAs increases as the external resistance increases. This is because at high external resistance the electron transfer through the circuit is limited by the resistance itself, at least in the initial phase of a feeding cycle. Electrons are extracted from the substrate quicker than they can be transferred to the electrode, thus they are preferentially diverted internally to PHB. A consequence of this fact is a difference in the growth pattern at different resistances. At 5 Ω growth on acetate prevails over PHB storage, thus growth happens primarily using acetate as carbon source; at 20 Ω PHB storage prevails over growth on acetate, therefore most growth occurs in the second part of the batch, using PHB as substrate; at 100 Ω the bacteria do not get enough energy for growth, and more than half of the substrate is stored within the cells as PHB before being oxidized.

Fermentation and Methanogenesis. This study is the first to provide a method to effectively quantify the effect of possible side-processes on the Coulombic efficiency of microbial fuel cells. Acetate is non fermentable, so it cannot produce hydrogen gas except in some specific conditions. As expected, no H₂ was found in the offgas. Also, the direct

conversion of acetate to methane is not competitive at the prevailing conditions in microbial fuel cell anodes. Contrarily, fermentation could be observed when the reactors were supplied with glucose. This was indicated by the liberation of hydrogen gas when glucose was fed to the acetate-adapted biofilm. When glucose was fed to the glucose-adapted biofilm, methane instead of hydrogen was found in the offgas. This indicates that the adaptation to glucose as substrate for several months enabled a significant development of a community of hydrogenotrophic methanogens. The amount of hydrogen observed in the offgas cannot be used to quantify the rate of fermentation of glucose, because part of the H₂ is expected to be oxidized directly at the anode (reaction 5); instead, it is simply an indicator that fermentation was occurring. Unlike what was previously reported (5), fermentation and methanogenesis appear to occur even at low external resistances. Fermentation and methanogenesis are not electrode-dependent reactions, so they could occur at any external resistance as long as the redox potential in the solution is low enough, and bacteria are present that gain more energy out of these processes than out of electrode driven substrate oxidation.

Acknowledgments

This research was supported by the Australian Research Council (Grant DP0666927).

Supporting Information Available

An explanation of the theoretical calculations of the growth and storage rates described in the Results section and the storage polymer visualization technique. This material is available free of charge via the Internet at <http://pubs.acs.org>.

Literature Cited

- (1) Rabaey, K.; Verstraete, W. Microbial fuel cells: novel biotechnology for energy generation. *Trends Biotechnol.* **2005**, *23* (6), 291–298.
- (2) Logan, B. E.; Hamelers, B.; Rozendal, R.; Schrorder, U.; Keller, J.; Freguia, S.; Aelterman, P.; Verstraete, W.; Rabaey, K. Microbial fuel cells: Methodology and technology. *Environ. Sci. Technol.* **2006**, *40* (17), 5181–5192.
- (3) Bond, D. R.; Holmes, D. E.; Tender, L. M.; Lovley, D. R. Electrode-reducing microorganisms that harvest energy from marine sediments. *Science* **2002**, *295* (5554), 483–485.

- (4) Chaudhuri, S. K.; Lovley, D. R. Electricity generation by direct oxidation of glucose in mediatorless microbial fuel cells. *Nat. Biotechnol.* **2003**, *21* (10), 1229–1232.
- (5) Rabaey, K.; Boon, N.; Siciliano, S. D.; Verhaege, M.; Verstraete, W. Biofuel cells select for microbial consortia that self-mediate electron transfer. *Appl. Environ. Microbiol.* **2004**, *70* (9), 5373–5382.
- (6) Park, D. H.; Zeikus, J. G. Impact of electrode composition on electricity generation in a single-compartment fuel cell using *Shewanella putrefaciens*. *Appl. Microbiol. Biotechnol.* **2002**, *59* (1), 58–61.
- (7) Oh, S. E.; Logan, B. E. Proton exchange membrane and electrode surface areas as factors that affect power generation in microbial fuel cells. *Appl. Microbiol. Biotechnol.* **2006**, *70* (2), 162–169.
- (8) Liu, H.; Logan, B. E. Electricity generation using an air-cathode single chamber microbial fuel cell in the presence and absence of a proton exchange membrane. *Environ. Sci. Technol.* **2004**, *38* (14), 4040–4046.
- (9) Rabaey, K.; Lissens, G.; Siciliano, S. D.; Verstraete, W. A microbial fuel cell capable of converting glucose to electricity at high rate and efficiency. *Biotechnol. Lett.* **2003**, *25* (18), 1531–1535.
- (10) Rabaey, K.; Ossieur, W.; Verhaege, M.; Verstraete, W. Continuous microbial fuel cells convert carbohydrates to electricity. *Water Sci. Technol.* **2005**, *52* (1–2), 515–523.
- (11) Pratt, S.; Yuan, Z. G.; Gapes, D.; Dorigo, M.; Zeng, R. J.; Keller, J. Development of a novel titration and off-gas analysis (TOGA) sensor for study of biological processes in wastewater treatment systems. *Biotechnol. Bioeng.* **2003**, *81* (4), 482–495.
- (12) Gapes, D.; Pratt, S.; Yuan, Z. G.; Keller, J. Online titrimetric and off-gas analysis for examining nitrification processes in wastewater treatment. *Water Res.* **2003**, *37* (11), 2678–2690.
- (13) Greenberg, A.; Clesceri, L. S.; Eaton, A. D. *Standard Methods for the Examination of Water and Wastewater*, 18th ed. American Public Health Association: Washington, DC, 1992.
- (14) van Aalst-van Leeuwen, M. A.; Pot, M. A.; van Loosdrecht, M. C. M.; Heijnen, J. J. Kinetic modeling of poly(beta-hydroxybutyrate) production and consumption by *Paracoccus pantotrophus* under dynamic substrate supply. *Biotechnol. Bioeng.* **1997**, *55* (5), 773–782.
- (15) Heijnen, J. J. Bioenergetics of microbial growth. In *Bioprocess Technology: Fermentation, Biocatalysis, Bioseparation*; Flickinger, M. C., Drew, S. W., Eds.; John Wiley and Sons: New York, 1999; pp 267–291.

Received for review October 30, 2006. Revised manuscript received February 8, 2007. Accepted February 13, 2007.

ES062611I